Asian Journal of Engineering and Applied Technology
ISSN: 2249-068X (P)
Vol.13 No.1, 2024, pp.8-19

www.crijournals.org
DOI: https://doi.org/10.70112/ajeat-2024.13.1.4236

Sawdust Ash as a Sustainable Binder in Geopolymer Concrete: A Study on Split Tensile Strength

Osere Gift, Nwofor Temple and Sule Samuel
Department of Civil Engineering, University of Port Harcourt, Port Harcourt, Nigeria
E-mail: oseregift2000@yahoo.com, templenwofor@gmail.com, samvictoryahead@yahoo.com
(Received 27 January 2024; Revised 20 February 2024; Accepted 8 March 2024; Available online 25 March 2024)

***Abstract* - Geopolymer concrete can serve as a more environmentally friendly alternative to traditional cement by reducing the release of greenhouse gases during production. It is composed of an alkaline liquid containing sodium or potassium silicate and sodium or potassium hydroxide, along with a source material rich in silica and alumina. In a recent investigation, thirty geopolymer concrete samples were created in the laboratory using a mix design approach. The study focused on optimizing the split tensile strength of the concrete, particularly when using sawdust ash as the source material. The research revealed that subjecting sawdust ash to pyrolysis in the absence of oxygen significantly affects its pozzolanic characteristics and, consequently, the properties of the concrete. The study determined the optimum split tensile strength of sawdust ash-blended geopolymer concrete to be 2.9899 MPa. The specific concentration ratios of NaOH, Na_2SiO_4 to NaOH, sawdust ash in the binder, water to binder, and activator to sawdust ash were found to be 9.75, 1.8750, 37.5, 0.025, and 2.5, respectively. Additionally, computer programs developed using MATLAB were employed to optimize and predict the ideal mix proportion of sawdust ash-based geopolymer concrete.**
Keywords: **Geopolymer Concrete, Sawdust Ash, Split Tensile Strength, Pyrolysis, MATLAB**

I. INTRODUCTION

For a significant period, ordinary Portland cement has been used as a binding agent in the production of ordinary Portland concrete (OPC). Increasing infrastructure demands in many emerging countries, along with a rise in the number of old, deteriorating concrete structures in urgent need of repair and rehabilitation, are contributing to the expected increase in demand for OPC. However, Mehta [1] revealed that the cement industry is responsible for almost seven percent (7%) of global greenhouse gas emissions and produces millions of tonnes of waste annually. More recently, Pearce [2] stated that anthropogenic greenhouse gas emissions from the cement industry account for 8% of the world's annual greenhouse gases. Consistent with the findings of Hardjito [3], the manufacturing of one metric tonne of Portland cement releases around one tonne of carbon dioxide (CO_2) into the environment.

The founder of the concept of geopolymer concrete, Davidovits [4], proposed creating binders by reacting silicon (Si) and aluminum (Al) in a geologically derived source material or by-product materials such as flue ash and rice husk ash. He named these binders "geopolymers" to represent the polymerization process involved in the chemical reaction. Geopolymer binders, an alternative to traditional cement, are created by combining pozzolanic precursors like flue ash and, in some cases, sawdust ash, which are rich in silica and alumina, with an alkaline solution to activate the process [5]-[9].

The cement industry cannot be classified as sustainable due to its reliance on raw materials obtained through mining, which negatively affects land use patterns. Moreover, the products manufactured by this industry are not recyclable. By taking waste management principles into account, the by-products of thermal power plants, such as flue ash, and the by-products of the steel industry, like slag, can be used as binders instead of cement. Furthermore, the by-product of the wood industry, sawdust, can also serve as a binder. This substitution has the potential to significantly reduce the energy needed for cement production. This approach can lead to energy conservation and a decrease in greenhouse gas emissions by saving both raw materials and energy resources within a specific limit. By incorporating this method, we can transform waste by-products into a practical and valuable substance, i.e., geopolymers in concrete.

In a study by Ivindra [10], the impact of the molarity of an alkaline activator solution (AAS) on the compressive strength of geopolymer concrete was explored. The study used NaOH solutions with concentrations of 10 M, 12 M, and 14 M and found that higher NaOH concentrations improved the compressive strength. The ideal NaOH concentration for geopolymer concrete was determined to be 12 M.

Jeremiah [11] examined the use of geopolymers made from industrial wastes such as PFA, GGBS, MK, GP, POFA, SF, RHA, VA, and MP for stabilizing weak clays. They found that the treated clays showed increased strength, making them suitable for road pavement construction. Other studies [12]-[18] have made notable contributions to the concepts of geopolymer concrete and its properties. Various guidelines, codes, standards, and specifications [19]-[28] were used in this work. The study aimed to determine the optimal mixture proportion of sawdust ash concrete geopolymers while also assessing the pozzolanic properties of sawdust ash and developing mathematical models and a MATLAB program for predicting and optimizing the split tensile strength of sawdust ash concrete geopolymers.

II. MATERIALS AND METHODS

A. Materials

The materials used in this study were all locally sourced within the City of Port Harcourt Metropolis. The following constituents were utilized in the study.

1. *Sawdust Ash:* The samples were obtained from the waste of wood treated in the Rumuosi sawmills over the course of a single day. Samples were collected from both hardwood and softwood sawdust. The collected samples were then converted into ash through open burning in a metal container and using an incinerator. Oxide composition tests and X-ray diffraction analysis (XRD) were performed on the samples to determine their pozzolanic properties and cementation characteristics.

2. *Water:* Clean tap water, free of impurities, color, and odor, was used. High impurity levels in the mixing water can lead to efflorescence, corrosion of reinforcement, and affect the setting time, concrete strength, and volume stability.

3. *Alkaline Liquid:* SiO_2 solutions and 8–14 M NaOH were used to activate the sawdust ash. The sodium silicate and sodium hydroxide were sourced from Mile 3 Market in Port Harcourt, Nigeria. The sodium hydroxide (NaOH) used in this research was dissolved in water at least six hours before mixing and had a purity level of 97–98 percent.

4. *Fine Aggregates:* The fine aggregate used in the study was sourced from the riverbank Choba sand dump. The clean, naturally occurring sand with rounded or sub-rounded particles was washed, sun-dried, and underwent a particle size distribution test before being used for concreting, adhering to BS 1881 [29] standards for grain size distribution.

5. *Coarse Aggregates:* Bags of coarse granite were collected from Mile 3 Market and brought to the lab for research purposes. Before being used for concreting, the granite was sun-dried and cleaned to remove impurities. Following this, a particle size distribution analysis was carried out. The research included the use of coarse aggregates of crushed granite with nominal maximum sizes of 7 mm, 10 mm, and 20 mm.

6. *Superplasticizer:* A superplasticizer utilizing naphthalene at a continuous dose of 1.25 percent of the binder weight was used in the concrete formulations. The primary aim of using this type of admixture was to achieve the desired slump. The admixture was purchased from Mile 3 Market in Port Harcourt, Rivers State, Nigeria.

B. Methods

The methods employed in this study comprise:

1. Experimental method
2. Mathematical model development

1. Experimental Method

The following laboratory tests were conducted for the geopolymer concrete derived from sawdust ash: particle size distribution, oxide composition test, specific gravity, density of constituent materials, and split tensile strength tests.

a. Sieve Analysis

i. Aggregate particle percentages of various sizes were calculated using sieve analysis.
ii. Standard BS 1881 [29] was followed for the sieve analysis.

(1) Fine Aggregate

i. A 1 kg test sample was dried at 110 ± 5°C.
ii. 52 g of oven-dried fine aggregate was used for sieve analysis; the sample was divided into two halves due to its higher mass.
iii. A mechanical shaker was used with sieves of 2.36 mm, 1.18 mm, 600 μm, 300 μm, and 150 μm.
iv. The weight of particles retained on each sieve was combined, and the fineness modulus was calculated.

(2) Coarse Aggregate

i. The same process as for fine aggregate was followed, as per BS 1881 [29].
ii. Sieving was done using mesh sizes of 26.5 mm, 19 mm, 9.5 mm, 4.75 mm, 2.36 mm, and 1.18 mm.
iii. The mass of the retained aggregate was recorded.

b. Specific Gravity and Density of Constituent Materials

Specific gravity and density of constituent materials, including sawdust ash, fine aggregates, and coarse aggregates, were determined in the laboratory and tabulated.

c. Split Tensile Resistance Test

Experimental measurements were taken of the concrete specimens' splitting tensile resistance in accordance with BS 1881 [29]. A 100 × 200 mm (diameter × height) cylinder was tested for splitting tensile resistance at 28 days old using the control MCC8 machine, which provided compressive force throughout the length of the cylinder. Cylinders underwent this test by having compressive line or strip loads applied along two opposed sides.

The vertical diametrical plane experienced almost homogeneous tensile stress under these conditions, causing the specimen to split or fracture along this plane. To determine any deviation from the ideal elastic assumption, this test utilized elastic stress analysis in conjunction with numerical approaches. At each age, two samples were checked, and the average resistance was recorded. Equations (3–8) were used to calculate the breaking tensile strength of the specimens.

$$F_{ct} = {}^{2P}/_{\pi LD} \quad (1)$$

Where;
F_{ct} = Indirect tensile Resistance (MPa),
P = Maximum applied force (kN),
L = Length of the specimens (mm),
D = Diameter of the Specimens (mm)

Fig. 1 A test of split tensile resistance is being done

2. Mathematical Model Development

a. Trial and Control Mixes

Scheffe, [30] states that Equation 2 can be used to calculate the sum of experimental data points.

$$N = \frac{(q+m-1)}{(q-1)!m!} \quad (2)$$

Where;
q = sum of the variables;
m = maximum summation of interactions

Keep the following information in mind:
For mixtures containing five and two components, the total number of experimental data points is fifteen (15) when Equation (2) is used.

The study used the following five ratios: activator/SDA, water/binder, percentage of SDA in binder, NaOH concentration (M), and Na_2SiO_4/NaOH ratio. The study utilized a simplex lattice design, as depicted in Figure 2.

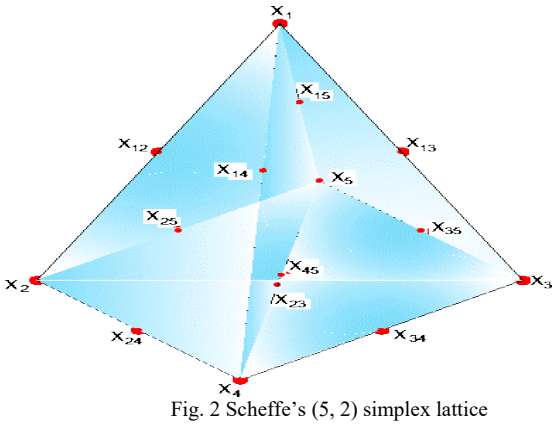

Fig. 2 Scheffe's (5, 2) simplex lattice

Scheffe [30] states that theoretical mix ratios, also known as pseudo mix ratios, are used to represent mixture proportions. At each vertex, there is a pure substance, and this approach assumes that the sum of all pseudo mix ratios is 1. From a mathematical standpoint, this method is employed to depict mixture compositions.

$$\sum_{i=1}^{q} x_i = 1 \quad (3)$$

To satisfy Equation (4), the actual mix ratios must be converted into pseudo mix ratios. The correlation between the two sets of mix ratios is as follows:

$$Z = [A]X \quad (4)$$

Where;
Z = column matrix of real constituent ratio.
X = column matrix of pseudo constituent ratio.
[A]= co-efficient matrix which is the transpose of the permutation matrix.

The matrix A is obtained by flipping the permutation matrix. The permutation matrix for NaOH concentration (M) ranged from 8M to 15M, resulting in a Na_2SiO_4/NaOH ratio between 1.5 and 3. The binder SDA content was limited to a range of 35% to 45%. The activator/SDA ratio fell within the range of 2.3 to 3.1, while the water/binder ratio was between 0 and 0.1. At the assumed pure substance points, the mix ratios are as follows: (8, 9.75, 11.5, 13.25, 15), (1.5, 1.875, 2.25, 2.625, 3), (35, 37.5, 40, 42.5, 45), (0, 0.025, 0.05, 0.075, 0.1), and (2.3, 2.485, 2.671, 2.856, 3.1). These points are represented by the permutation matrix [P0].

$$P_o = \begin{bmatrix} 8 & 1.5 & 35 & 0 & 2.3 \\ 9.75 & 1.875 & 37.5 & 0.025 & 2.485 \\ 11.5 & 2.25 & 40 & 0.005 & 2.671 \\ 13.25 & 2.625 & 42.5 & 0.075 & 2.856 \\ 15 & 3 & 45 & 0.1 & 3.1 \end{bmatrix}$$

Transpose of Po becomes

$$A = \begin{bmatrix} 8 & 9.75 & 11.5 & 13.25 & 15 \\ 1.5 & 1.875 & 2.25 & 2.625 & 3 \\ 35 & 37.5 & 40 & 42.5 & 45 \\ 0 & 0.025 & 0.05 & 0.075 & 0.1 \\ 2.3 & 2.485 & 2.671 & 2.856 & 3.1 \end{bmatrix}$$

Specifically, the ensuing are the pseudo mix proportions of the center or interaction sites from Figure 2.

$$X = \begin{bmatrix} 1 & 0 & 0 & 0 & 0 & 0.5 & 0.5 & 0.5 & 0.5 & 0 & 0 & 0 & 0 & 0 & 0 \\ 0 & 1 & 0 & 0 & 0 & 0.5 & 0 & 0 & 0 & 0.5 & 0.5 & 0.5 & 0 & 0 & 0 \\ 0 & 0 & 1 & 0 & 0 & 0 & 0.5 & 0 & 0 & 0.5 & 0 & 0 & 0.5 & 0.5 & 0 \\ 0 & 0 & 0 & 1 & 0 & 0 & 0 & 0.5 & 0 & 0 & 0.5 & 0 & 0.5 & 0 & 0.5 \\ 0 & 0 & 0 & 0 & 1 & 0 & 0 & 0 & 0.5 & 0 & 0 & 0.5 & 0 & 0.5 & 0.5 \end{bmatrix}$$

The trail mix matrix, Z, becomes;

$$Z = \begin{bmatrix} 8 & 9.75 & 11.5 & 13.25 & 15 & 8.875 & 9.75 & 10.625 & 11.5 & 10.625 & 11.5 & 12.375 & 12.375 & 13.25 & 14.125 \\ 1.5 & 1.875 & 2.25 & 2.625 & 3 & 1.6875 & 1.875 & 2.0625 & 2.25 & 2.0625 & 2.25 & 4.4375 & 2.4375 & 2.625 & 2.8125 \\ 35 & 37.5 & 40 & 42.5 & 45 & 36.25 & 37.5 & 38.75 & 40 & 38.75 & 40 & 41.25 & 41.25 & 42.5 & 43.75 \\ 0 & 0.025 & 0.05 & 0.075 & 0.1 & 0.0125 & 0.025 & 0.0375 & 0.05 & 0.0375 & 0.05 & 0.0625 & 0.0625 & 0.075 & 0.0875 \\ 2.3 & 2.485 & 2.671 & 2.856 & 3.1 & 2.3925 & 2.4855 & 2.578 & 2.7 & 2.578 & 2.6705 & 2.7925 & 2.7635 & 2.8855 & 2.978 \end{bmatrix}$$

Tables I below represent the trial mix matrix of SDA concrete mixes respectively after proper application of Equation 5.

TABLE I TRIAL MIX MATRIX POINTS OWING TO SCHEFFE'S (5, 2) FACTOR SPACE

N	Pseudo Constituent					Actual Constituent				
	X_1	X_2	X_3	X_4	X_5	Z1 = NaOH conc. (M)	Z2 = Na2SiO4/ NaOH	Z3 = percent SDA in binder	Z4 = water/binder	Z5 = Activator/ SDA
1	1	0	0	0	0	8	1.5	35	0	2.3
2	0	1	0	0	0	9.75	1.875	37.5	0.025	2.485
3	0	0	1	0	0	11.5	2.25	40	0.05	2.671
4	0	0	0	1	0	13.25	2.625	42.5	0.075	2.856
5	0	0	0	0	1	15	3	45	0.1	3.1
6	½	½	0	0	0	8.875	1.6875	36.25	0.0125	2.3925
7	½	0	½	0	0	9.75	1.875	37.5	0.025	2.4855
8	½	0	0	½	0	10.625	2.0625	38.75	0.0375	2.578
9	½	0	0	0	½	11.5	2.25	40	0.05	2.7
10	0	½	½	0	0	10.625	2.0625	38.75	0.0375	2.578
11	0	½	0	½	0	11.5	2.25	40	0.05	2.6705
12	0	½	0	0	½	12.375	2.4375	41.25	0.0625	2.7925
13	0	0	½	½	0	12.375	2.4375	41.25	0.0625	2.7635
14	0	0	½	0	½	13.25	2.625	42.5	0.075	2.8855
15	0	0	0	½	½	14.125	2.8125	43.75	0.0875	2.978

Similarly, for the control mix matrix, the pseudo mix proportion adopted in line with Scheffe's criteria is given as;

$$Xc = \begin{bmatrix} \frac{1}{3} & \frac{1}{3} & \frac{1}{3} & \frac{1}{3} & \frac{1}{4} & \frac{1}{4} & \frac{1}{4} & 0 & \frac{3}{10} & \frac{1}{5} & \frac{1}{5} & \frac{1}{5} & \frac{3}{20} & \frac{1}{5} & \frac{1}{4} \\ \frac{1}{3} & \frac{1}{3} & 0 & \frac{1}{3} & \frac{1}{4} & \frac{1}{4} & \frac{1}{4} & \frac{1}{4} & \frac{1}{10} & \frac{1}{5} & \frac{1}{5} & \frac{1}{5} & \frac{1}{4} & \frac{1}{5} & \frac{1}{5} \\ \frac{1}{3} & 0 & \frac{1}{3} & 0 & \frac{1}{4} & \frac{1}{4} & 0 & \frac{1}{4} & \frac{1}{5} & \frac{1}{10} & \frac{1}{5} & \frac{1}{5} & \frac{1}{5} & \frac{3}{20} & \frac{1}{5} \\ 0 & \frac{1}{3} & \frac{1}{3} & 0 & \frac{1}{4} & 0 & \frac{1}{4} & \frac{1}{4} & \frac{1}{5} & \frac{3}{10} & \frac{3}{10} & \frac{1}{5} & \frac{1}{5} & \frac{1}{4} & \frac{1}{5} \\ 0 & 0 & 0 & \frac{1}{3} & 0 & \frac{1}{4} & \frac{1}{4} & \frac{1}{4} & \frac{1}{5} & \frac{1}{5} & \frac{1}{10} & \frac{1}{5} & \frac{1}{5} & \frac{1}{5} & \frac{3}{20} \end{bmatrix}$$

Multiplying the pseudo mix proportions for control, X_c by A, the control mix matrix, Z_c, becomes;

$$Zc = \begin{bmatrix} 9.75 & 10.33 & 10.92 & 10.92 & 10.63 & 11.06 & 11.50 & 12.38 & 11.33 & 11.68 & 11.33 & 11.50 & 11.59 & 11.59 & 11.15 \\ 1.88 & 2.00 & 2.13 & 2.13 & 2.06 & 2.16 & 2.25 & 2.44 & 2.21 & 2.29 & 2.21 & 2.25 & 2.27 & 2.27 & 2.18 \\ 37.50 & 38.33 & 39.17 & 39.17 & 38.75 & 39.38 & 40.00 & 41.25 & 39.75 & 40.25 & 39.75 & 40.00 & 40.13 & 40.13 & 39.50 \\ 0.03 & 0.03 & 0.04 & 0.04 & 0.04 & 0.04 & 0.05 & 0.06 & 0.05 & 0.05 & 0.05 & 0.05 & 0.05 & 0.05 & 0.05 \\ 2.49 & 2.55 & 2.61 & 2.63 & 2.58 & 2.64 & 2.69 & 2.78 & 2.66 & 2.70 & 2.66 & 2.68 & 2.69 & 2.69 & 2.64 \end{bmatrix}$$

The control mix design matrix and the trial mix design for concrete that are geopolymers adopted in this study is given in Table II and Table III respectively.

TABLE II CONTROL MIX MATRIX OWING TO SCHEFFE'S (5, 2) FACTOR SPACE

N	Pseudo Constituent					Actual Constituent				
	X_1	X_2	X_3	X_4	X_5	Z_1 = NaOH conc. (M)	Z_2 = Na2SiO4/ NaOH	Z_3 = percent SDA in binder	Z_4 = water/binder	Z_5 = Activator/ SDA
1	1/3	1/3	1/3	0	0	9.75	1.88	37.50	0.03	2.49
2	1/3	1/3	0	1/3	0	10.33	2.00	38.33	0.03	2.55
3	1/3	0	1/3	1/3	0	10.92	2.13	39.17	0.04	2.61
4	1/3	1/3	0	0	1/3	10.92	2.13	39.17	0.04	2.63
5	¼	¼	¼	¼	0	10.63	2.06	38.75	0.04	2.58
6	¼	¼	¼	0	¼	11.06	2.16	39.38	0.04	2.64
7	¼	¼	0	¼	¼	11.50	2.25	40.00	0.05	2.69
8	0	¼	¼	¼	¼	12.38	2.44	41.25	0.06	2.78
9	3/10	1/10	1/5	1/5	1/5	11.33	2.21	39.75	0.05	2.66
10	1/5	1/5	1/10	3/10	1/5	11.68	2.29	40.25	0.05	2.70
11	1/5	1/5	1/5	3/10	1/10	11.33	2.21	39.75	0.05	2.66
12	1/5	1/5	1/5	1/5	1/5	11.50	2.25	40.00	0.05	2.68
13	3/20	¼	1/5	1/5	1/5	11.59	2.27	40.13	0.05	2.69
14	1/5	1/5	3/20	¼	1/5	11.59	2.27	40.13	0.05	2.69
15	¼	1/5	1/5	1/5	3/20	11.15	2.18	39.50	0.05	2.64

TABLE III TRIAL MIX DESIGN OF SAWDUST ASH GEOPOLYMER CONCRETE

Sl. No.	Mix ID	Conc. Of NaOH (M)	SS/SH	Activator/ SDA	Super-Plasticizers (percent of Binder)	Binder (Kg)	percent of SDA in Binder	SDA (Kg)	SAND (Kg)	Aggregates (Kg)	Water/ Binders
1	GPC1	8	1.5	2.3	0.05	2.1	35	0.74	4.1	8.2	0
2	GPC2	9.75	1.875	2.485	0.05	2.1	37.5	0.79	4.1	8.2	0.025
3	GPC3	11.5	2.25	2.671	0.05	2.1	40	0.84	4.1	8.2	0.05
4	GPC4	13.25	2.625	2.856	0.05	2.1	42.5	0.89	4.1	8.2	0.075
5	GPC5	15	3	3.10	0.05	2.1	45	0.95	4.1	8.2	0.1
6	GPC6	8.875	1.6875	2.39	0.05	2.1	36.25	0.76	4.1	8.2	0.0125
7	GPC7	9.75	1.875	2.49	0.05	2.1	37.5	0.79	4.1	8.2	0.025
8	GPC8	10.625	2.0625	2.58	0.05	2.1	38.75	0.81	4.1	8.2	0.0375
9	GPC9	11.5	2.25	2.70	0.05	2.1	40	0.84	4.1	8.2	0.05
10	GPC10	10.625	2.0625	2.58	0.05	2.1	38.75	0.81	4.1	8.2	0.0375
11	GPC11	11.5	2.25	2.67	0.05	2.1	40	0.84	4.1	8.2	0.05
12	GPC12	12.375	2.4375	2.79	0.05	2.1	41.25	0.87	4.1	8.2	0.0625
13	GPC13	12.375	2.4375	2.76	0.05	2.1	41.25	0.87	4.1	8.2	0.0625
14	GPC14	13.25	2.625	2.89	0.05	2.1	42.5	0.89	4.1	8.2	0.075
15	GPC15	14.125	2.8125	2.98	0.05	2.1	43.75	0.92	4.1	8.2	0.0875

b. Optimization Model Development

It has been previously established that mixture proportions are represented by theoretical mix ratios based on Scheffe's (5,2) simplex lattice. It is also understood that pure substances exist at the vertices, and the method relies on the condition that the sum of all theoretical mix ratios at any point must equal 1. This explains the constraint in the optimization process, as shown in Equation (3).

The (q, m) polynomial have a general form represented by Equation 5 (Scheffe, 1958);

$$Y = b_o + \Sigma b_i x_i + \Sigma b_{ij} x_i x_j + \Sigma b_{ijk} x_i x_j x_k + \cdots + \Sigma b_{i1,i2..im} x_{i1} x_{i2} x_{im} \quad (5)$$

Where; $1 \le i \le q$, $1 \le i \le j \le q$, $1 \le i \le j \le k \le q$

b_o is a constant coefficient

For (5, 2) polynomial problem as adopted in this study, Equation (5) becomes;

$$Y = b_0 + b_1X_1 + b_2X_2 + b_3X_3 + b_4X_4 + b_5X_5 + b_{12}X_{12}X_2 + b_{13}X_1X_3 + b_{14}X_1X_4 + b_{15}X_1X_5 + b_{25}X_2X_5 +$$

$$b_{24}X_2X_4 + b_{23}X_2X_3 + b_{34}X_3X_4 + b_{35}X_3X_5 + b_{45}X_4X_5 + b_{11}X_1^2 + b_{22}X_2^2 + b_{33}X_3^2 + b_{44}X_4^2 + b_{55}X_5^2 \quad (6)$$

For a ternary mixture, Equation (7) is obtained from Equation (3).

$$X_1 + X_2 + X_3 + X_4 + X_5 = 1 \quad (7)$$

Multiplying through by constant, b_0, yields Equation (8).

$$b_0X_1 + b_0X_2 + b_0X_3 + b_0X_4 + b_0X_5 = b_0 \quad (8)$$

Again, multiplying Equation (8) by X_1, X_2, X_3, X_4 and X_5 in succession and rearranging, Equation (9) is produced.

$$\left.\begin{aligned} X_1^2 &= X_1 - X_1X_2 - X_1X_3 - X_1X_4 - X_1X_5 \\ X_2^2 &= X_2 - X_1X_2 - X_2X_3 - X_2X_4 - X_2X_5 \\ X_3^2 &= X_3 - X_1X_3 - X_2X_3 - X_3X_4 - X_3X_5 \\ X_4^2 &= X_4 - X_1X_4 - X_2X_4 - X_3X_4 - X_4X_5 \\ X_5^2 &= X_5 - X_1X_5 - X_2X_5 - X_3X_5 - X_4X_5 \end{aligned}\right\} \quad (9)$$

Substituting Equations (8) and (9) into Equation (6), Equation (10) was obtained after necessary transformation.

$$\begin{aligned} Y = {} & (b_0 + b_1 + b_{11})X_1 + (b_0 + b_2 + b_{22})X_2 \\ & + (b_0 + b_3 + b_{33})X_3 \\ & + (b_0 + b_4 + b_{44})X_4 \\ & + (b_0 + b_5 + b_{55})X_5 \\ & + (b_{12} - b_{11} - b_{22})X_1X_2 \\ & + (b_{13} - b_{11} - b_{33})X_1X_3 \\ & + (b_{14} - b_{11} - b_{44})X_1X_4 \\ & + (b_{15} - b_{11} - b_{55})X_1X_5 \\ & + (b_{23} - b_{22} - b_{33})X_2X_3 \\ & + (b_{24} - b_{22} - b_{44})X_2X_4 \\ & + (b_{25} - b_{22} - b_{55})X_2X_5 \\ & + (b_{34} - b_{33} - b_{44})X_3X_4 \\ & + (b_{35} - b_{33} - b_{55})X_3X_5 \\ & + (b_{45} - b_{44} - b_{55})X_4X_5 \end{aligned} \quad (10)$$

Denoting; $\beta_i = b_0 + b_i + b_{ii}$ and
$\beta_{ij} = b_{ij} - b_{ii} - b_{jj}$

With five variables, the simplified second-degree polynomial may be seen in Equation (11).

$$\begin{aligned} Y = {} & \beta_1X_1 + \beta_2X_2 + \beta_3X_3 + \beta_4X_4 + \beta_5X_5 + \beta_{12}X_1X_2 \\ & + \beta_{13}X_1X_3 + \beta_{14}X_1X_4 + \beta_{15}X_1X_5 \\ & + \beta_{23}X_2X_3 + \beta_{24}X_2X_4 + \beta_{25}X_2X_5 + \beta_{34}X_3X_4 + \beta_{35}X_3X_5 + \\ & \beta_{45}X_4X_5 \end{aligned} \quad (11)$$

Equation (11) uses fifteen (15) coefficients instead of the numerous coefficients found in Equation (6). Therefore, Equation (12) represents the reduced second-degree polynomial in q-variables.

$$Y = \sum_{1\le i\le q} \beta_i X_i + \sum_{i\le j\le q} \beta_{ij} X_iX_j \quad (12)$$

Where;

Y = Expected response
β_i, β_{ij} = Co-efficient of the quadratic polynomial
X_i, X_j = Pseudo proportion of factors considered

Equation (13) is obtained by substituting the coordinates of the vertices from Figure 2 into Equation (9).

$$\left.\begin{aligned} Y_1 &= \beta_1 \\ Y_2 &= \beta_2 \\ Y_3 &= \beta_3 \\ Y_4 &= \beta_4 \\ Y_5 &= \beta_5 \end{aligned}\right\} \quad (13)$$

For interaction point X_{12} of Figure 2;

$$\begin{aligned} Y_{12} &= {}^1/_2 X_1 + {}^1/_2 X_2 + {}^1/_4 X_1X_2 \\ &= {}^1/_2 \beta_1 + {}^1/_2 \beta_2 + {}^1/_4 \beta_{12} \end{aligned} \quad (14)$$

In congruent with Equation (7), β_i is equal to Y_i, where i ranges from 1 to n. By plugging the values into Equation (8), the ensuing upshot was obtained:

$$Y_{12} = ({}^1/_2)Y_1 + ({}^1/_2)Y_2 + ({}^1/_4)\beta_{12} \quad (15)$$

Simplifying Equation (15), yielded:

$$B_{12} = 4Y_{12} - 2Y_1 - 2Y_2 \quad (16)$$

Equations (17) to (20) were derived in a similar manner. Therefore:

$$B_{13} = 4Y_{13} - 2Y_1 - 2Y_3 \quad (17)$$
$$B_{14} = 4Y_{14} - 2Y_1 - 2Y_4 \quad (18)$$
$$B_{15} = 4Y_{15} - 2Y_1 - 2Y_5 \quad (19)$$
$$B_{23} = 4Y_{23} - 2Y_2 - 2Y_3 \quad (20)$$

By generalizing equations (16) to (20), equation (21) was derived.

$$\left.\begin{aligned} \beta_i &= Y_i \\ \beta_{ij} &= 4Y_{ij} - 2Y_i - 2Y_j \end{aligned}\right\} \quad (21)$$

The numbers mentioned above are utilized as the co-efficient for the second-degree polynomial with coordinates (5, 2) in Equation (9).

c. Optimization Models Validation

To validate and ensure appropriateness, the models generated using Equation (11) were subjected to the Fisher test (F-test). The F-statistic compares the variance of the experimental values with the expected model response values. The hypotheses were accepted to validate the models.

Null Hypothesis:
H_0 = there exist no substantial difference between the experimental and calculated responses.

Alternate Hypothesis:
H_1= there is a substantial difference between the experimental and calculated responses.

The F-test may be expressed mathematically as Equation (22).

$$F = \frac{S_1^2}{S_2^2} \quad (22)$$

Where; S_1^2 = Larger of both variances
S_2^2 = Smaller of both variances

S2 is calculated utilizing the ensuing equation:

$$S^2 = \frac{1}{n-1}[\sum(Y - \bar{Y})^2] \quad (23)$$

Where: $\bar{Y}$= Average mean of response, Y
Y = Mean of response

For the models to be considered sufficient, the F-values computed using Equation (22) must be smaller than the values reported in the F-distribution table.

III. RESULTS AND DISCUSSION

A. Results

The results of the tests on constituent materials, fifteen (15) trial runs of geopolymer concrete mixtures, and fifteen (15) control mixes for split tensile strength are presented and discussed in this section.

TABLE IV OXIDE COMPOSITION TEXT

Chemical Properties Parameter	Hardwood Sawdust Ash		Softwood Sawdust Ash	
	Sample 1 (With Oxygen)	Sample 2 (Without Oxygen)	Sample 3 (With Oxygen)	Sample 4 (Without Oxygen)
CaO (%)	6.13	4.18	5.46	5.11
SiO2 (%)	69.84	71.02	66.79	72.57
Al2O3 (%)	3.78	4.32	4.81	5.16
Fe2O3 (%)	1.94	1.82	2.27	2.36
MgO (%)	3.20	3.47	4.10	4.43
Na_2O (%)	0.28	0.19	0.11	0.15
K2O (%)	2.95	3.11	2.88	3.28
Loss of Ignition	2.92	3.11	3.56	3.44

Table IV displays the results of the oxide composition test conducted on softwood and hardwood sawdust ash. The test revealed that softwood sawdust ash, produced through pyrolysis, exhibits superior pozzolanic properties and was therefore selected for further laboratory investigation. The X-ray diffraction (XRD) test conducted on the sawdust ash sample further supported the decision to use softwood sawdust ash.

Tables V(a)-V(d) provide the specific gravity and density of sawdust ash and fine aggregate, indicating their suitability for further testing.

TABLE V (a) SPECIFIC GRAVITY OF SAWDUST ASH

Bottle/Test Number		1	2
Weight of Bottle only(g) -	M_1	28.0	26.5
Weight of Bottle and dry sample(g) -	M_2	36.0	35.0
Weight of Bottle, sample and water(g) -	M_3	82.0	80.0
Weight of Bottle and water(g) -	M_4	78.0	78.0
$G_s = M_2 - M_1/(M_4 - M_1) - (M_3 - M_2)$		2.0	1.308
Average(Gs)		1.654	

TABLE V (b) SPECIFIC GRAVITY OF FINE AGGREGATE

Bottle/Test Number		1	2
Weight of Bottle only(g) -	M_1	28.0	26.5
Weight of Bottle and dry sample(g) -	M_2	64	64.5
Weight of Bottle, sample and water(g) -	M_3	102	100
Weight of Bottle and water(g) -	M_4	78.0	78.0
$G_s = M_2 - M_1/(M_4 - M_1) - (M_3 - M_2)$		3.0	2.375
Average(Gs)		2.6875	

TABLE V (c) DENSITY OF SAWDUST ASH

Volume of Mould		$2.2 * 10^{-4} m^3$	
Test		1	2
Wt. of Specimen + Mould	gms	678.0	776.0
Wt. of Mould only	gms	444.0	444.0
Wt. of Specimen	gms	234.0	332.0
Density of Specimen	g/m^3	1.045	1.482
Average Density	g/m^3	1.2635	
Bulk Density	Kg/m^3	1.2635	
Unit Weight	KN/m^3	12.609	

TABLE V (d) DENSITY OF FINE AGGREGATE

Volume of Mould		$2.2 * 10^{-4} m^3$	
Test		1	2
Wt. of Specimen + Mould	gms	864.0	872.0
Wt. of Mould only	gms	444.0	444.0
Wt. of Specimen	gms	420.0	428.0
Density of Specimen	g/m^3	1.875	1.910
Average Density	g/m^3	1.8925	
Bulk Density	kg/m^3	1.8925	
Unit Weight	KN/m^3	18.560	

Table VI presents the split tensile strength results obtained from laboratory experiments using the trial mix design specified in Table III. In these experiments, the geopolymer binder completely replaced cement, while the fine and coarse aggregates remained constant throughout the testing. Other factors, such as rest period, superplasticizer, and curing temperature, were also kept constant. The samples were cured in an oven at 90°C for three days and then aged for 28 days before being subjected to crushing.

TABLE VI SPLIT TENSILE STRENGTH OF SAWDUST ASH GEOPOLYMER CONCRETE EXPERIMENTAL RESULT FOR TRIAL MIXES AT 28 DAYS CURING AGE

N	Pseudo constituent					Actual constituent					Response	
	X_1	X_2	X_3	X_4	X_5	Z_1 = NaOH conc. (M)	Z_2 = Na2SiO4/ NaOH	Z_3 = percent SDA in binder	Z_4 = water/binder	Z_5 = Activator/ SDA	Symbol	Split Tensile Strength (N/mm^2)
1	1	0	0	0	0	8	1.5	35	0	2.3	Y_1	2.956
2	0	1	0	0	0	9.75	1.875	37.5	0.025	2.485	Y_2	2.413
3	0	0	1	0	0	11.5	2.25	40	0.05	2.671	Y_3	2.956
4	0	0	0	1	0	13.25	2.625	42.5	0.075	2.856	Y_4	2.413
5	0	0	0	0	1	15	3	45	0.1	3.1	Y_5	2.685
6	½	½	0	0	0	8.875	1.6875	36.25	0.0125	2.3925	Y_{12}	2.685
7	½	0	½	0	0	9.75	1.875	37.5	0.025	2.4855	Y_{13}	2.413
8	½	0	0	½	0	10.625	2.0625	38.75	0.0375	2.578	Y_{14}	2.685
9	½	0	0	0	½	11.5	2.25	40	0.05	2.7	Y_{15}	2.956
10	0	½	½	0	0	10.625	2.0625	38.75	0.0375	2.578	Y_{23}	2.685
11	0	½	0	½	0	11.5	2.25	40	0.05	2.6705	Y_{24}	2.956
12	0	½	0	0	½	12.375	2.4375	41.25	0.0625	2.7925	Y_{25}	2.956
13	0	0	½	½	0	12.375	2.4375	41.25	0.0625	2.7635	Y_{34}	2.956
14	0	0	½	0	½	13.25	2.625	42.5	0.075	2.8855	Y_{35}	2.413
15	0	0	0	½	½	14.125	2.8125	43.75	0.0875	2.978	Y_{45}	1.707

B. Modeling the Split Tensile Strength of Sawdust Ash Geopolymer Concrete

The split tensile test results for the trial mix of geopolymer concrete are presented in Table VI. This table, along with Equation (11), was used to derive the model coefficients for Scheffe's (5, 2) optimization models for the split tensile strength of geopolymer concrete incorporating sawdust ash. The optimization model for Scheffe's (5, 2) split tensile resistance of sawdust ash-blended geopolymer concrete is developed as follows.

$\beta_1 = Y_1 = 2.956$
$\beta_2 = Y_2 = 2.413$
$\beta_3 = Y_3 = 2.956$
$\beta_4 = Y_4 = 2.413$
$\beta_5 = Y_5 = 2.685$

$$\beta_{12} = 4Y_{12} - 2Y_1 - 2Y_2 = 4(2.685) - 2(2.956) - 2(2.413) = 0.002$$

$$\beta_{13} = 4Y_{13} - 2Y_1 - 2Y_3 = 4(2.413) - 2(2.956) - 2(2.956) = -2.172$$

$$\beta_{14} = 4Y_{14} - 2Y_1 - 2Y_4 = 4(2.685) - 2(2.956) - 2(2.413) = 0.002$$

$$\beta_{15} = 4Y_{15} - 2Y_1 - 2Y_5 = 4(2.956) - 2(2.956) - 2(2.685) = 0.542$$

$$\beta_{23} = 4Y_{23} - 2Y_2 - 2Y_3 = 4(2.685) - 2(2.413) - 2(2.956) = 0.002$$

$$\beta_{24} = 4Y_{24} - 2Y_2 - 2Y_4 = 4(2.956) - 2(2.413) - 2(2.413) = 2.172$$

$$\beta_{25} = 4Y_{25} - 2Y_2 - 2Y_5 = 4(2.956) - 2(2.413) - 2(2.685) = 1.628$$

$$\beta_{34} = 4Y_{34} - 2Y_3 - 2Y_4 = 4(2.956) - 2(2.956) - 2(2.413) = 1.086$$

$$\beta_{35} = 4Y_{35} - 2Y_3 - 2Y_5 = 4(2.413) - 2(2.956) - 2(2.685) = -1.630$$

$$\beta_{45} = 4Y_{45} - 2Y_4 - 2Y_5 = 4(1.707) - 2(2.413) - 2(2.685) = -3.368$$

The above equation enables the substitution of the aforementioned coefficient values to forecast the optimum mixture proportions for sawdust ash-based geopolymer concrete, based on split tensile strength, using the optimization model.

$$Y = 2.956x_1 + 2.413x_2 + 2.956x_3 + 2.413x_4 + 2.685x_5 + 0.002x_1x_2 - 2.172x_1x_3 + 0.002x_1x_4 + 0.542x_1x_5 + 0.002x_2x_3 + 2.172x_2x_4 + 1.628x_2x_5 + 1.086x_3x_4 - 1.630x_3x_5 - 3.368x_4x_5 \quad (24)$$

Equation (24) represents the (5, 2) optimization model used to estimate the split tensile resistance of sawdust ash-blended geopolymer concrete. This model can be employed to predict the split tensile resistance of sawdust ash concrete for any

desired value within the range of split tensile strength values obtained from the trial mix.

Using MATLAB code developed for this research, the modified pseudo coefficients, x1 to x5, were obtained. These values can also be determined using Excel Solver.

X_1	X_2	X_3	X_4	X_5	$\sum x$
0.75	0	0	0	0.25	1

Substituting the optimal pseudo coefficients into Equation (24), the optimum split tensile strength for the sawdust ash-based geopolymer concrete is determined as follows:

$$Y_{op} = 3.3002$$

Applying the modified pseudo coefficients, the optimized mix design for sawdust ash-blended geopolymer concrete is provided in Table VII.

TABLE VII SPLIT TENSILE STRENGTH OPTIMUM MIX DESIGN FOR SAWDUST ASH BASED GEOPOLYMER CONCRETE

Pseudo Constituent					**Actual Constituent**					**Optimum Split Tensile resistance (N/mm^2)**
X_1	**X_2**	**X_3**	**X_4**	**X_5**	Z_1 = **NaOH conc. (M)**	Z_2 = **Na2SiO4/ NaOH**	**Z_3 = percent SDA in binder**	Z_4 = **water/ binder**	Z_5 = **Activator/ SDA**	
0.75	0	0	0	0.25	9.7500	1.8750	37.5	0.0250	2.5000	2.9899

C. Validation and Verification of Optimization Model

Adequacy tests were conducted using F-statistics and verification tests using R^2 statistics on the optimization models developed in the previous section. This part of the study utilized the split tensile resistance laboratory response values for the control mix design matrix in Table II. Table VIII presents the experimental results for the split tensile resistance of the control mix. The average split tensile resistance values in Table VIII are compared with the predicted values shown in Table IX. These predicted values are calculated by substituting the pseudo matrix for the control mix from Table II into the previously developed optimization model (Equation 24). Figure 2 provides a graphical representation (R^2 statistics) comparing the predicted values with the control mix values in Table IX, used to determine the R^2 value. Finally, Table X shows the F-statistics validation, used to calculate the variances between the experimental and predicted values.

TABLE VIII CONTROL MIX SPLIT TENSILE STRENGTH EXPERIMENTAL RESULTS AT 28 DAYS CURING AGE

N	**Pseudo Constituent**					**Actual Constituent**					**Response Symbol**	**Split Tensile. Resistance (N/mm^2)**		**Average Split Tensile resistance (N/mm^2)**
	X_1	**X_2**	**X_3**	**X_4**	**X_5**	Z_1 = **NaOH conc. (M)**	Z_2 = **Na2SiO4/ NaOH**	**Z_3 = percent SDA in binder**	Z_4 = **water/binder**	Z_5 = **Activator/ SDA**		**Sample 1**	**Sample 2**	
1	1/3	1/3	1/3	0	0	9.75	1.88	37.50	0.03	2.49	Y_1	2.580	2.737	2.658
2	1/3	1/3	0	1/3	0	10.33	2.00	38.33	0.03	2.55	Y_2	2.956	2.811	2.884
3	1/3	0	1/3	1/3	0	10.92	2.13	39.17	0.04	2.61	Y_3	2.737	2.737	2.737
4	1/3	1/3	0	0	1/3	10.92	2.13	39.17	0.04	2.63	Y_4	2.885	3.025	2.955
5	¼	¼	¼	¼	0	10.63	2.06	38.75	0.04	2.58	Y_5	2.737	2.885	2.811
6	¼	¼	¼	0	¼	11.06	2.16	39.38	0.04	2.64	Y_{12}	2.580	2.811	2.696
7	¼	¼	0	¼	¼	11.50	2.25	40.00	0.05	2.69	Y_{13}	2.885	2.737	2.811
8	0	¼	¼	¼	¼	12.38	2.44	41.25	0.06	2.78	Y_{14}	2.580	2.774	2.677
9	3/10	1/10	1/5	1/5	1/5	11.33	2.21	39.75	0.05	2.66	Y_{15}	2.580	2.774	2.677
10	1/5	1/5	1/10	3/10	1/5	11.68	2.29	40.25	0.05	2.70	Y_{23}	2.659	2.811	2.735
11	1/5	1/5	1/5	3/10	1/10	11.33	2.21	39.75	0.05	2.66	Y_{24}	2.737	2.811	2.774
12	1/5	1/5	1/5	1/5	1/5	11.50	2.25	40.00	0.05	2.68	Y_{25}	2.774	2.580	2.677
13	3/20	¼	1/5	1/5	1/5	11.59	2.27	40.13	0.05	2.69	Y_{34}	2.811	2.737	2.774
14	1/5	1/5	3/20	¼	1/5	11.59	2.27	40.13	0.05	2.69	Y_{35}	2.737	2.737	2.737
15	¼	1/5	1/5	1/5	3/20	11.15	2.18	39.50	0.05	2.64	Y_{45}	2.659	2.811	2.735

TABLE IX COMPARISON OF PREDICTED SPLIT TENSILE STRENGTH VALUES WITH THE EXPERIMENTAL VALUES

N	Pseudo Constituent					Actual Constituent					Response Symbol	Split Tensile. Resistance (N/mm²)	
	X_1	X_2	X_3	X_4	X_5	Z_1 = NaOH conc. (M)	Z_2 = Na2SiO4/ NaOH	Z_3 = percent SDA in binder	Z_4 = water/binder	Z_5 = Activator/ SDA		Experiment Upshot	Calculated Value
1	1/3	1/3	1/3	0	0	9.75	1.88	37.50	0.03	2.49	Y_1	2.658	2.534
2	1/3	1/3	0	1/3	0	10.33	2.00	38.33	0.03	2.55	Y_2	2.884	2.835
3	1/3	0	1/3	1/3	0	10.92	2.13	39.17	0.04	2.61	Y_3	2.737	2.654
4	1/3	1/3	0	0	1/3	10.92	2.13	39.17	0.04	2.63	Y_4	2.955	2.926
5	¼	¼	¼	¼	0	10.63	2.06	38.75	0.04	2.58	Y_5	2.811	2.752
6	¼	¼	¼	0	¼	11.06	2.16	39.38	0.04	2.64	Y_{12}	2.696	2.651
7	¼	¼	0	¼	¼	11.50	2.25	40.00	0.05	2.69	Y_{13}	2.811	2.677
8	0	¼	¼	¼	¼	12.38	2.44	41.25	0.06	2.78	Y_{14}	2.677	2.610
9	3/10	1/10	1/5	1/5	1/5	11.33	2.21	39.75	0.05	2.66	Y_{15}	2.677	2.561
10	1/5	1/5	1/10	3/10	1/5	11.68	2.29	40.25	0.05	2.70	Y_{23}	2.735	2.602
11	1/5	1/5	1/5	3/10	1/10	11.33	2.21	39.75	0.05	2.66	Y_{24}	2.774	2.676
12	1/5	1/5	1/5	1/5	1/5	11.50	2.25	40.00	0.05	2.68	Y_{25}	2.677	2.615
13	3/20	¼	1/5	1/5	1/5	11.59	2.27	40.13	0.05	2.69	Y_{34}	2.774	2.642
14	1/5	1/5	3/20	¼	1/5	11.59	2.27	40.13	0.05	2.69	Y_{35}	2.737	2.611
15	¼	1/5	1/5	1/5	3/20	11.15	2.18	39.50	0.05	2.64	Y_{45}	2.735	2.639

Where; X_1, Z_1= pseudo and actual constituent of NaOH concentration; X2, Z2 = pseudo and actual constituent of Na2SiO4/NaOH ratio; X3, Z3 = pseudo and Actual constituent of percent of SDA in binder; X4, Z4 = pseudo and actual constituent of water/binder ratio; X5, Z5 = pseudo and actual constituent of Activator/SDA ratio.

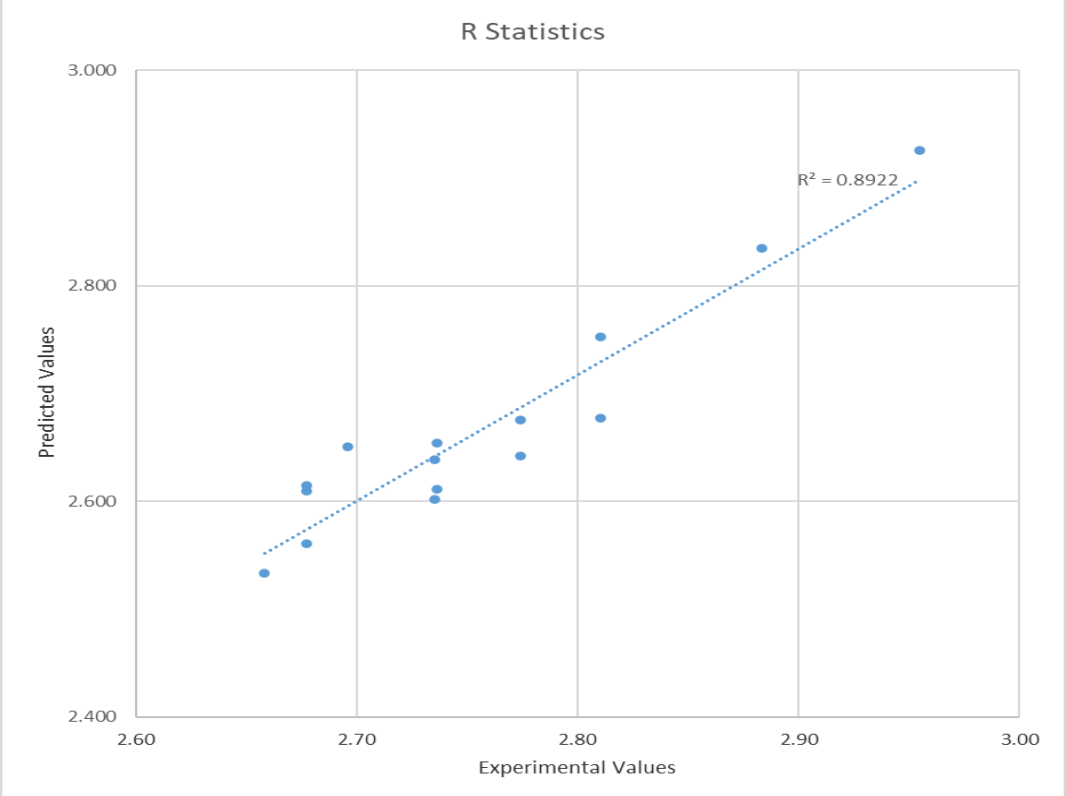

Fig. 2 R^2 Statistics of sawdust ash blended geopolymer concrete Split Tensile Strength model

TABLE X F-STATISTICS FOR VALIDATION OF SAWDUST ASH CONCRETE THAT ARE GEOPOLYMERS SPLIT TENSILE STRENGTH OPTIMIZATION MODEL

Experiment Value = Y_e	Pred. value = Y_m	Y_e-$\hat{Y}_e$	Y^m-$\hat{Y}^m$	$(Y_e$-$\hat{Y}_e)^2$	$(Y^m$-$\hat{Y}^m)^2$
2.6583	2.5339	-0.0975	-0.1317	0.0095	0.0173
2.8836	2.8352	0.1278	0.1696	0.0163	0.0288
2.7365	2.6544	-0.0193	-0.0112	0.0004	0.0001
2.9549	2.9256	0.1991	0.2600	0.0396	0.0676
2.8105	2.7524	0.0547	0.0868	0.0030	0.0075
2.6957	2.6507	-0.0601	-0.0149	0.0036	0.0002
2.8105	2.6773	0.0547	0.0117	0.0030	0.0001
2.6771	2.6095	-0.0787	-0.0561	0.0062	0.0031
2.6771	2.5606	-0.0787	-0.1050	0.0062	0.0110
2.7354	2.6017	-0.0204	-0.0639	0.0004	0.0041
2.7740	2.6757	0.0182	0.0101	0.0003	0.0001
2.6771	2.6149	-0.0787	-0.0507	0.0062	0.0026
2.7740	2.6420	0.0182	-0.0236	0.0003	0.0006
2.7365	2.6110	-0.0193	-0.0546	0.0004	0.0030
2.7354	2.6391	-0.3066	-0.0265	0.0940	0.0007
$\hat{Y}_e$ = 2.7559	$\hat{Y}^m$ =2.6659			$\sum$= 0.0962	$\sum$= 0.1471

With the aid of Table X and Equation (23) the following was deduced:

$$S_e^2 = {}^{0.0962}/_{14} = 0.0069$$
$$S_m^2 = {}^{0.1479}/_{14} = 0.0105$$

The F-value which is the ratio of the two squared variances was computed using Equation (22) as;

$$F = {}^{0.0105}/_{0.0069} = 1.5287$$

The calculated F-value (F-cal) is 1.5287, which is less than the tabulated F-value (F-tab) of 2.4986. Therefore, we accept the null hypothesis, and the model is considered adequate.

Additionally, the R2 statistics shown in Figure 2 indicate an R2 value of 89.22%. This suggests that over 89% of the dataset is explained by the optimization model.

IV. CONCLUSION

Based on the experimental work reported in this study, several key conclusions were drawn. First, sawdust ash demonstrates superior pozzolanic properties when subjected to pyrolysis in the absence of oxygen, as opposed to burning in the presence of oxygen. This indicates that the pyrolysis process enhances the reactivity of the ash, making it more effective as a pozzolanic material. Furthermore, it was observed that softwood sawdust is more effective in this regard compared to hardwood sawdust, suggesting that the type of wood used in the production of sawdust ash significantly influences the resulting material's properties. Additionally, a mathematical formulation has been developed to predict the split tensile strength of geopolymer concrete derived from sawdust ash, providing a valuable tool for optimizing and forecasting the performance of this sustainable construction material.

$$Y = 2.956x_1 + 2.413x_2 + 2.956x_3 + 2.413x_4 + 2.685x_5 + 0.002x_1x_2 - 2.172x_1x_3 + 0.002x_1x_4 + 0.542x_1x_5 + 0.002x_2x_3 + 2.172x_2x_4 + 1.628x_2x_5 + 1.086x_3x_4 - 1.630x_3x_5 - 3.368x_4x_5.$$

The study revealed several important findings regarding the behavior and properties of sawdust ash-based geopolymer concrete. It was observed that the fresh concrete could be easily handled for up to 120 minutes without any signs of setting or degradation in split tensile strength, indicating good workability. However, an increase in the H_2O-to-Na_2O molar ratio resulted in a decrease in split tensile strength, suggesting that careful control of this ratio is crucial for optimizing strength. Similarly, increasing the water-to-geopolymer solids ratio by mass also led to a reduction in split tensile strength. Interestingly, the Na_2O-to-SiO_2 molar ratio did not significantly impact the split tensile strength, indicating that this parameter may be less critical in the mix design. Additionally, the split tensile strength of heat-cured sawdust ash-based geopolymer concrete was found to be independent of age, implying that the strength is largely determined during the curing process. Prolonged mixing time, up to 16 minutes, was shown to enhance the split tensile strength, suggesting that extended mixing could be beneficial. Finally, the average density of sawdust ash-based geopolymer concrete was found to be comparable to that of ordinary Portland cement (OPC) concrete, highlighting its potential as a sustainable alternative to traditional concrete.

REFERENCES

[1] P. K. Mehta, "Reducing the Environmental Impact of Concrete," *Concrete International*, vol. 23, no. 3, pp. 61-66, 2001.

[2] F. Pearce, "At Climate Summit: Can the World's Most Polluting Heavy Industries Decarbonize?" *Yale Environment 360*, Yale School of Environment, 2021. [Online]. Available: https://e360.yale.edu/features/at-glasgow-can.

[3] D. Hardjito and B. V. Rangan, "Development and Properties of Low-Calcium Fly Ash-Based Geopolymer Concrete," Research Report GC1, Faculty of Engineering, Curtin University of Technology, Perth, 2005. [Online]. Available: espace@curtin or www.geopolymer.org.

[4] J. Davidovits, "Geopolymers: Inorganic Polymeric New Materials," *Journal of Thermal Analysis and Calorimetry*, vol. 37, pp. 1633-1656, 1991.

[5] I. Luhar and S. Luhar, "A Comprehensive Review on Fly Ash-Based Geopolymer," *Journal of Composites Science*, vol. 6, no. 8, p. 219, 2019.

[6] K. A. Anuar, A. R. M. Ridzuan, and S. Ismail, "Strength Characteristic of Geopolymer Concrete," *International Journal of Civil & Environmental Engineering*, vol. 11, no. 1, pp. 59-62, 2011.

[7] R. Anuradha, V. Sreevidya, R. Venkatasubramani, and B. V. Rangan, "Modified Guidelines for Geopolymer Concrete Mix Design Using Indian Standards," *Asian Journal of Civil Engineering*, vol. 13, no. 3, pp. 353-364, 2012.

[8] J. Davidovits, "Chemistry of Geopolymer Systems, Terminology, Geopolymer," *International Conference*, France, vol. 99, pp. 3077-3085, 1998.

[9] D. Hardjito, E. Wallah, D. M. J. Sumajouw, and B. V. Rangan, "Factors Influencing the Compressive Strength of Fly Ash-Based Geopolymer Concrete," *Civil Engineering Dimension*, vol. 6, no. 2, pp. 88–93, 2004.

[10] P. Ivindra, H. Herwani, I. Iswandi, and B. Bambang, "Compressive Strength of Fly Ash-Based Geopolymer Concrete with a Variable of Sodium Hydroxide (NaOH) Solution Molarity," *MATEC Web of Conferences*, vol. 147, p. 01004, 2018.

[11] J. J. Jeremiah, J. Samuel, C. A. B., and A. K. Anil, "Geopolymers as Alternative Sustainable Binders for Stabilisation of Clays—A Review," *Journal of Geotechnics*, vol. 1, pp. 439–459, 2021.

[12] M. Mageswari and B. Vidivelli, "The Use of Saw Dust Ash as Fine Aggregate Replacement in Concrete," *Journal of Environmental Research and Development*, vol. 3, no. 3, pp. 720-726, 2009.

[13] C. Marthong, "Sawdust Ash (SDA) as Partial Replacement of Cement," *International Journal of Engineering Research and Applications*, vol. 2, no. 4, pp. 1980-1985, 2012.

[14] A. M. A. Mohd, W. H. Mohd, and R. B. M. Aamer, "Mix Design and Compressive Strength of Geopolymer Concrete Containing Blended Ash from Agro-Industrial Wastes," *Journal of Advanced Materials Research*, vol. 339, pp. 452-457, 2011.

[15] A. M. M. Nuru, H. Kamarudin, R. A. Rafiza, T. A. F. Meor, and M. Rosnita, "Compressive Strength of Fly Ash Geopolymer Concrete by Varying Sodium Hydroxide Molarity and Aggregate to Binder Ratio," *2nd Joint Conference on Green Engineering Technology & Applied Computing*, 2020.

[16] G. P. Suresh and Manojkumar, "Factors Influencing Compressive Strength of Geopolymer Concrete," *International Journal of Research in Engineering and Technology*, vol. 3, no. 4, pp. 13-31, 2013.

[17] J. Davidovits, "Properties of Geopolymer Cements," in *Alkaline Cements and Concretes*, Kiev State Technical University, Kiev, Ukraine, vol. 1, pp. 131-149, 1994.

[18] J. Davidovits, "Fire Proof Geopolymer Cements," in *Geopolymer 99 Proceedings: Second International Conference*, France, vol. 99, pp. 165-169, 1999.

[19] R. Anuradha, V. Sreevidya, R. Venkatasubramani, and B. V. Rangan, "Modified Guidelines for Geopolymer Concrete Mix Design Using Indian Standards," *Asian Journal of Civil Engineering*, vol. 13, no. 3, pp. 353-364, 2012.

[20] M. Sofi, J. S. J. van Deventer, P. A. Mendis, and G. C. Lukey, "Bond Performance of Reinforcing Bars in Inorganic Polymer Concrete (IPC)," *Journal of Materials Science*, vol. 42, pp. 3107–3116, 2007.

[21] P. J. Tikalsky and R. L. Carrasquillo, "Influence of Fly Ash on the Sulfate Resistance of Concrete," *ACI Materials Journal*, vol. 89, no. 1, pp. 69-75, 1992.

[22] J. G. S. Van Jaarsveld, J. S. J. van Deventer, and G. C. Lukey, "The Effect of Composition and Temperature on the Properties of Fly Ash- and Kaolinite-Based Geopolymers," *Chemical Engineering Journal*, vol. 89, no. 1-3, pp. 63-73, 2002.

[23] R. I. Gilbert, "Creep and Shrinkage Models for High Strength Concrete - Proposal for Inclusion in AS3600," *Australian Journal of Structural Engineering*, vol. 4, no. 2, pp. 95-106, 2002. [Online]. Available: http://search.informit.com.au/documentSummary;dn=289028371180229;res=IELENG.

[24] L. Zuda, Z. Pavlik, P. Rovnanikova, P. Bayer, and R. Cerny, "Properties of Alkali Activated Aluminosilicate Material After Thermal Load," *International Journal of Thermophysics*, vol. 27, no. 4, pp. 1250-1263, 2006.

[25] ASTM C618-05, "Standard Specification for Coal Fly Ash and Raw or Calcined Natural Pozzolan for Use as a Mineral Admixture in Concrete," American Society for Testing and Materials International, West Conshohocken, Philadelphia, 2005.

[26] EN 1992-1-1, "Eurocode 2: Design of Concrete Structures," European Commission.

[27] IS 3812:1981, "Indian Standard Specification for Fly Ash for Use as Pozzolana and Admixture."

[28] IS 383:1970, "Specification for Coarse and Fine Aggregates from Natural Sources for Concrete."

[29] BS 1881-2, "Methods of Testing Fresh Concrete," British Standards Institution, 1970.

[30] H. Scheffé, "Experiments with Mixtures," *Journal of the Royal Statistical Society: Series B*, vol. 20, pp. 344-360, 1958.